Parametrically forced, breaking gravity waves in a circular cylinder

S. P. Das, E. J. Hopfinger and Estelle Guyez[+]

LEGI/CNRS, B.P. 53, 38041 Grenoble Cedex
emil.hopfinger@hmg.inpg.fr
+ CME Dept., University of Warwick, Coventry, UK

Abtract :

In this paper we present results on parametrically forced gravity waves in a circular cylinder in the limit of large fluid depth. The phase diagram that shows the stability threshold forcing amplitude and the wave breaking threshold has been determined in a frequency range near the natural frequency of the lowest axi-symmetric wave mode. The wave amplitude response curve, at forcing amplitude below the onset of wave breaking, exhibits wave amplitude modulations and bifurcations to other wave modes of frequency close to the axi-symmetric mode frequency. In the unstable regime a finite time singularity occurs with intense geyser or jet formation, a phenomenon demonstrated by Zeff et al. (2000) in fluids of high viscosity. Here this singularity is demonstrated for a low viscosity and low surface tension liquid.

Résumé :

Nous présentons des résultats sur des ondes de gravité créées par instabilité paramétrique dans un réservoir cylindrique et dans la limite d'eau profonde. Le diagramme de phase établi pour des fréquences proches du premier mode axisymétrique montre le seuil d'instabilité ainsi que le seuil d'existence d'ondes stables. L'amplitude des ondes en fonction de la fréquence d'excitation, déterminée pour une amplitude d'excitation en dessous du seuil d'instabilité des ondes, montre des modulations de l'amplitude des ondes ainsi que des bifurcations vers des modes asymétriques. Dans le régime des ondes instables une singularité en temps fini se produit, donnant naissance à des jets à grande vitesse, un phénomène démontré par Zeff et al. (2000) dans des fluides visqueux. Ici une telle singularité est montrée dans des fluides de faible viscosité et faible tension de surface.

Key-words : gravity waves, parametric instability, geyser formation

1 Introduction

Parametrically forced surface waves, known as Faraday waves, that are sub-harmonically excited, have been studied rather extensively (Benjamin & Ursell 1954; Kumar & Tuckermann, 1994, Edwards & Fauve, 1994). However, far less is known about large amplitude waves and wave breaking conditions especially of gravity waves. Large amplitude sloshing in containers is encountered in rocket engine fuel tanks and ship tanks. In these applications it is important to be able to predict the forces exerted by the sloshing motion on the tank walls as well as the consequences of sloshing and wave breaking on interfacial heat and mass transfer. Experimental results on sloshing due to horizontal forcing of circular and square-base cylindrical containers have been reported by Royon-Lebeaud et al. (2007). Here we present results on sloshing when the container is subjected to vertical (along the axis) motions. Vertical forcing allows exciting axi-symmetric as well as asymmetric wave modes depending on forcing frequency.

Parametrically forced gravity waves and the breaking scenarios in two-dimensions have been studied by Jiang et al. (1998). Breaking occurs when the wave amplitude has reached a value such that the downward acceleration of the wave crest is equal or slightly larger than the gravity. In a circular cylinder, axi-symmetric wave breaking can be much more violent and geyser formation is possible (Zeff et al. 2000). Henderson & Miles (1990), from here on referred to as HM, determined the stability

conditions and the steady-state wave amplitude of the axi-symmetric wave mode in a "small" circular cylinder. Small implies that dissipation is important.

In this paper we present results on parametrically forced gravity waves in a circular cylinder of size similar to the one of HM but using a fluid with low kinematic viscosity and low surface tension so that dissipation remains small. We first compare the experimental stability space of forcing amplitude as a function of wave frequency with theoretical predictions taking into account surface tension and viscosity corrections according to HM. This stability space is then compared with wave breaking threshold in the forcing amplitude-wave frequency domain. The wave amplitude response curves, obtained for the same frequency domain, exhibit the existence of steady-state wave motion. In the unstable regime, of the axi-symmetric mode (0,1) a finite time singularity can occur with intense jet formation, a phenomenon demonstrated by Zeff et al. (2000) in fluids of high viscosity. Here this singularity is shown to exist in fluids of low viscosity and low surface tension; in water it is less pronounced because of the large surface tension causing capillary wave perturbations.

2 Experimental conditions

The experiments have been conducted in a circular, cylindrical test cell, 5 cm in diameter and 6 cm in height that is mounted on a vertically vibrating table that is used in the frequency range 10 to 14 Hz and vibration amplitudes A= 0 to 1 mm. In the container used, the sub-harmonically excited axi-symmetric gravity wave mode has a wave number $k_{01}R$=3.832. The interesting aspect of parametrically forced waves is the close neighbourhood of the asymmetric wave modes (2,1), (3,1), (1,2), (4,1); the wave motion will lock to the mode of frequency $\omega/2$ with lowest dissipation. The container is filled to a depth h=3 cm with a low viscosity and low surface tension liquid, FC-72, of ν = 0.00406 cm^2/s, σ =11.5 dyn/cm and ρ =1.69Kg/m^3 at 20°C. The liquid depth is sufficient to satisfy $tanh(k_{01}h) \cong 1$ (asymptotically deepwater conditions). The container acceleration $a(t) = A\omega^2 \sin \omega t$ used in the experiments is $a(t) \leq 5$ m/s^2 and the forcing frequency (Hz) covered is $10.8 \leq \omega/2\pi \leq 13.6$.

Because of the small size of the container measurements were made by visualizations and image analysis only. Generally, a digital camera with an acquisition speed of 60 frames/second (fps) was used. Near resonant conditions with high velocity geyser formation, images were also taken with a high-speed camera at 1000 fps.

3 Theoretical concepts

The theory of weakly non-linear axi-symmetric wave motion in a circular cylinder (taking into account viscous effects) has been developed by HM following Miles (1984). The dispersion relation with surface tension added is of the form

$$\omega_{mn}^2 = g k_{mn}\left(1+\frac{k_{mn}^2\sigma}{g\rho}\right)\tanh(k_{mn}h)\,. \qquad (1)$$

The boundary condition on the container wall is that the velocity potential ϕ is $\partial\phi/\partial r\big|_{r=R} = J_m'(k_{mn}R) = 0$ which gives for the axi-symmetric wave modes, n =1 and 2, $k_{01}R$=3.8317 and $k_{02}R$= 5.3314 and for the asymmetric modes $k_{21}R$ = 3.0542, $k_{31}R$ = 4.2012, $k_{41}R$ = 5.3176. The corresponding natural frequencies are given by (1). For FC-72 and the container of R=2.5cm filled to a depth, h=3cm, the natural frequency of mode (0,1) is 39.090 rad s^{-1}.

The natural frequency shift due to linear damping is $\hat{\omega}_{mn} = \omega_{mn}(1-\delta)$ where $\delta = \kappa / \widehat{\omega}_{nm}$ is the damping ratio and κ the damping rate. Viscous dissipation in the Stokes boundary layer dominates over bulk dissipation. HM give the following analytical expression for deep water and a free surface without rigidity:

$$\delta = \frac{1}{2R}\left(\frac{\nu}{2\omega_{mn}}\right)^{1/2}\frac{1+(m/k_{mn}R)^2}{1-(m/k_{mn}R)^2} \tag{2}$$

Using the dispersion relation (1) and neglecting surface tension terms, (2) can be written in the form

$$\delta = C_1(\nu^2/R^3 g)^{1/4}, \tag{3}$$

where the coefficient C_1, a function of the wave mode as indicated by (2). Its value predicted by (2) is about a factor of 2 less than the values determined from experiments (Section 4.1).

In the theory of HM the steady-state wave amplitude as a function of time (at a given spatial position) depends on a small parameter ε, that is for the axi-symmetric mode

$$\varepsilon = Ak_{01}\tanh(k_{01}h), \tag{4}$$

and on the frequency offset parameter

$$\beta = \frac{(\omega/2)^2 - \hat{\omega}_{01}^2}{2\varepsilon\hat{\omega}_{01}^2} \tag{5}$$

Steady-state waves exist in the range $-\gamma < \beta < \gamma$, where

$$\gamma = \left[1-(\delta/\varepsilon)^2\right]^{1/2} \tag{6}$$

Neutral stability is given by $\beta = \pm\gamma$, with corresponding threshold forcing amplitude:

$$\frac{A}{R} = \frac{1}{3.832\tanh(3.832h/R)}\left[\delta^2 + \frac{\left((\omega/2)^2 - \hat{\omega}_{01}^2\right)^2}{(2\hat{\omega}_{01}^2)^2}\right]^{1/2} \tag{7}$$

4 Results

4.1 Damping coefficient

For the determination of the instability threshold it is important to know the damping coefficient δ with good accuracy. When the wave amplitude was established, the forcing was stopped and the wave motion decayed freely in time. Since the damping rate is small, the decay is exponential and is of the form $b = b_0\exp(-\delta\omega t)$, where b_0 is the wave amplitude at the stop of the forcing. Taking images of the wave motion at 60fps, corresponds to a sampling frequency of about ten times the wave frequency. By interpolation the wave motion was reconstructed giving the successive wave amplitudes to an accuracy of about 3%. For the wave mode k_{01}, the damping coefficient is $\delta \cong 0.01$ and corresponds to $C_1 \cong 1.75$ in (3). This value was used in calculating the instability threshold from (7). Using the relation $\hat{\omega}_{01} = \omega_{01}(1-\delta)$, the natural frequency of the axi-symmetric mode after viscosity correction is $\hat{\omega}_{01} = 38.699$ rad s^{-1}. From here on we drop the hat ($\hat{\omega}_{01} \equiv \omega_{01}$).

4.2 Instability and wave breaking thresholds

Figure 1a shows the non-dimensional forcing amplitudes of the instability and wave breaking thresholds as a function of non-dimensional frequency $\omega/2\omega_{01}$. The solid line corresponds to (7), with $\delta = 0.01$. There is good agreement between the experimental and calculated instability thresholds in the range $1.02 < \omega/2\omega_{01} < 0.96$. For $\omega/2\omega_{01} > 1.02$ the experimental values deviate substantially from the theoretical ones because the excited wave mode is k_{31}. In general, there is a large difference between the instability threshold forcing amplitude and wave breaking threshold,

except when $0.94<\omega/2\omega_{01}<0.969$ where the two overlap and breaking always occurs just above the instability threshold; in this range no stable waves exist. Figure 1a shows clearly that the limits of existence of stable wave motion depend on both, the forcing frequency and forcing amplitude related by the frequency-offset parameter $\beta=\frac{(\omega/2)^2-\omega_{01}^2}{2\varepsilon\omega_{01}^2}$. The frequency domain of existence of wave breaking increases with forcing amplitude. The onset of wave breaking is at $\varepsilon = 0.0322$ giving $\beta = -\gamma = 0.951$. The corresponding dimensionless forcing frequency obtained from (8) is 0.969:

$$\frac{\omega}{2\omega_{01}}=\left(-\left\{1-(\delta/\varepsilon)^2\right\}^{1/2}2\varepsilon+1\right)^{1/2} \qquad (8)$$

4.3 Wave amplitude response

Figure 1b shows the wave amplitude response *b/R* as a function of dimensionless frequency $\omega/2\omega_{01}$ for forcing amplitude *A/R*=0.006. All experimental points correspond to stable wave motions. The closed symbols indicate the existence of the axi-symmetric mode (0,1) and the open symbols refer to mode (3,1) when $\omega/2\omega_{01}>1.02$ and to mode (2,1) when $\omega/2\omega_{01}<0.97$. Stable axi-symmetric wave motions are indeed observed for $-\gamma < \beta < \gamma$ but near $-\gamma$ there is an amplitude modulation.

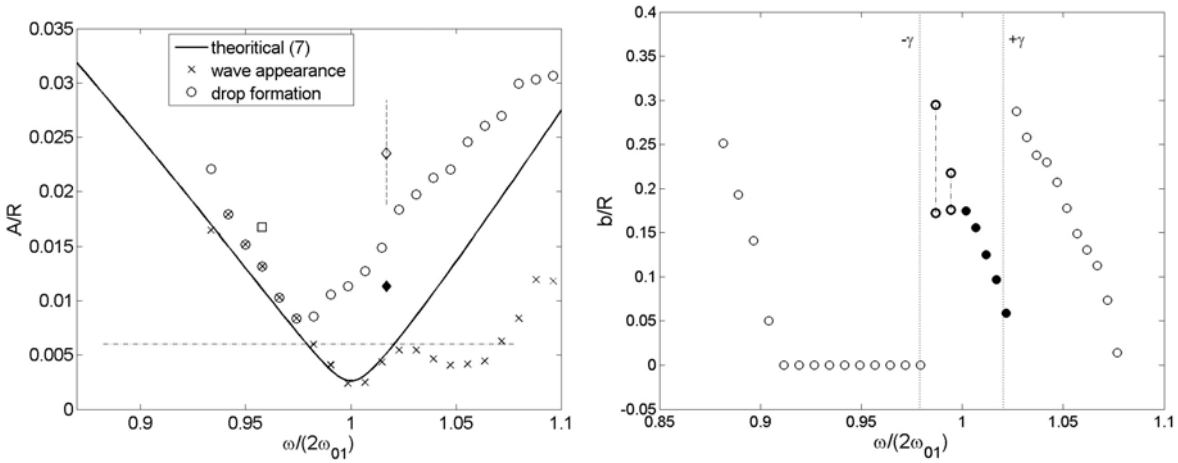

(a) (b)

Figure 1: (a) Instability and wave breaking threshold amplitudes A_c/R (×) and A_d/R (o) as a function of $\omega/2\omega_{01}$. The symbols □ and ◊ in the plot correspond respectively to *A/R*=0.0167, $\omega/2\omega_{01}$ = 0.96 and *A/R*=0.0235, $\omega/2\omega_{01}$=1.017 at which the images of geyser formation shown in Figure 2 were obtained. The symbol ♦ and the vertical dashed line refer to conditions at which the jet velocity has been measured (Figure 3). (b) Wave amplitude response for forcing amplitude, *A/R* = 0.006, indicated by horizontal dashed line in (a). Open, light symbols are for the asymmetric modes and the closed symbols are for the axi-symmetric mode. Open, thick symbols indicate the range of the wave amplitude modulation. The dash-dotted vertical lines connecting the same symbols give the magnitude of the amplitude modulations and the dotted vertical lines indicate the limits $-\gamma < \beta < \gamma$.

4.4 Jet formation

For container forcing amplitudes $A > A_d$ wave breaking occurs. Axi-symmetric wave mode breaking occurs via a high velocity geyser or jet formation. The geyser is formed by the collapse of the depression of the large amplitude axi-symmetric standing wave, a phenomenon referred to as finite-time singularity (Zeff et al. 2000). Images of the wave depression (lower part of image) and of geyser

formation (upper part of image) are shown in Figures 2a and 2b for two different forcing conditions; these conditions are indicated in figure 1a by the symbols □ and ◊.

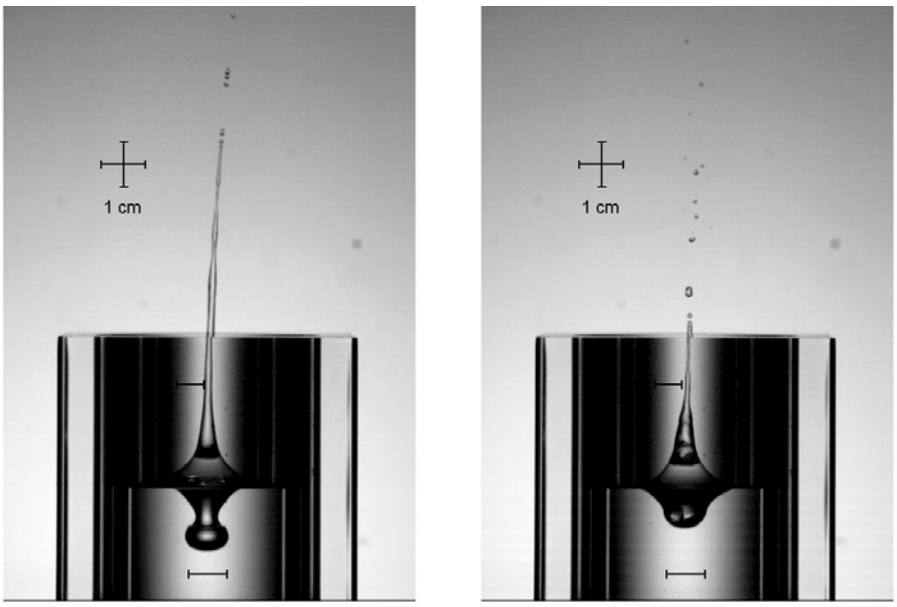

(a) (b)

Figure 2. A composite of two photographs showing the axi-symmetric standing wave depression below and geyser formation above for (a), *A/R*=0.0167, $\omega/2\omega_{01}$ =0.96; (b), *A/R*=0.0235, $\omega/2\omega_{01}$=1.017. The horizontal and vertical bars represent 1cm. The horizontal scale changes with location because of optical distortions.

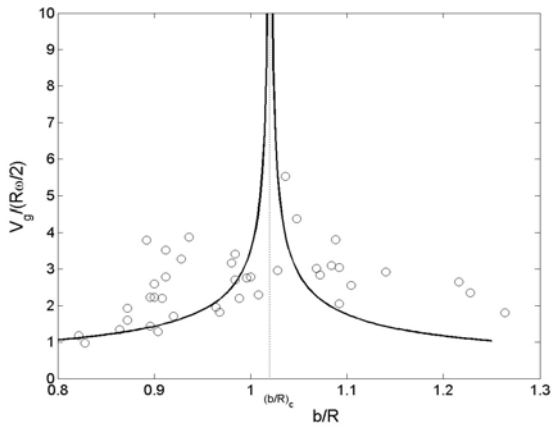

Figure 3. Normalised jet velocity, $V_g/(R\omega/2)$, vs. the last smooth standing wave height for $\omega/2\omega_{01}=1.017$. A steady-state wave motion was first established at *A/R* = 0.012 (symbol ♦ in figure 1a) and then the forcing amplitude was increased above the wave breaking threshold. The solid line is obtained from the Weber number correlation. The vertical, dotted line indicates the critical value of the last stable standing wave height $(b/R)_c \cong 1.02$. $R\omega/2$=98.37cm s^{-1}.

Zeff et al. developed a similarity theory and a power law scaling in $(t-t_0)^{\pm 2/3}$ of the free surface displacement and the velocity potential (where t_0 is the time of singularity) to calculate the form of the free surface depression near t_0. The scaling introduces a Weber number and the experiments of Zeff et al. seem to indicate that the maximum geyser velocity.

V_g scales with a Weber number in the form $We = \rho V_g^2 (b - b_c)/\sigma$, where b_c is the stable wave amplitude above which bubble pinch-off (Figure 2a) takes place. The value of the critical Weber number is not given but their experimental results suggest a value of $We_c \approx 4000$. The container radius should enter in the scaling because the critical wave amplitude b_c must depend on R. Viscous cut-off prevents V_g from becoming infinite as $b \to b_c$. A non-smooth surface has a similar cut-off effect as viscosity. This is the case with water where perturbations in the form of parasitic capillary waves appear. Zeff et al. used a glycerin-water solution of ν=1.94 cm^{2}s^{-1} to keep the surface smooth at large wave amplitudes. For the fluid used in the present experiments parasitic capillary waves are not a problem because of the low surface tension. Figure 3 shows the normalised velocity of the jet as a function of b/R. The ratio of the critical wave amplitude to radius is $(b/R)_c \cong 1.02$ and We=4000. When the jet velocity and wave amplitude are appropriately scaled, the Weber number relation is $\frac{V_g^2}{(R\omega/2)^2} = 4000 \frac{\sigma}{\rho} \frac{1}{R(R\omega/2)^2} \frac{R}{b\left(1 - \frac{b_c}{b}\right)}$. This is shown by the solid lines in Figure 3.

5 Conclusions

The experimentally determined stability threshold of the parametrically forced axi-symmetric gravity wave mode in low viscosity and low surface tension fluid in a circular cylinder is shown to be in good agreement with the HM theory. Bifurcations to other wave modes take place when the forcing frequency approaches the natural frequency of these modes. Stable wave motions exist between the stability threshold and the wave-breaking threshold established in the present experiments. The amplitude response curve shows that in a certain frequency range these stable waves exhibit amplitude modulations. In the unstable regime, a finite time singularity occurs with intense geyser or jet formation, a phenomenon demonstrated by Zeff et al. (2000) in fluids of high viscosity. Here this singularity is demonstrated for a low viscosity and low surface tension liquid. A dimensionless expression for the jet velocity is proposed that takes into account the container size in addition to the fluid properties.

Acknowledgements

The valuable help of Deepak Singh during preliminary experiments is gratefully acknowledged. The work was financially supported by contract CNS n° 60167 within the COMPERE program.

References

Benjamin, T. B. & Ursell, F., 1954, The stability of plane free surface of a liquid in a vertical periodic motion. *Proc. R. Soc. Lond. A*, **225**, 505-515.

Edwards, W.S. & Fauve, S., 1994, Patterns and quasi-patterns in the Faraday experiment. *J. Fluid Mech.*, **278**, 123–148.

Henderson, D. M. & Miles, J. W., 1990, Single-mode Faraday waves in small cylinders. *J. Fluid Mech.* **213**, 95-109.

Jiang, L., Perlin, M. & Schultz, W. W., 1998, Period tripling and energy dissipation of breaking standing waves. *J. Fluid Mech.*, **369**, 273-299.

Kumar, K. & Tuckerman, L. S., 1994, Parametric instability of the interface between two fluids. *J. Fluid Mech.*, **279**, 49-68.

Miles, J. W., 1984, Resonantly forced surface waves in a circular cylinder. *J. Fluid Mech.*, **149**, 15-31.

Royon-Lebeaud, A. Hopfinger, E.J. & Cartellier, A. 2007, Liquid sloshing and wave breaking in circular and square-base cylindrical containers. *J.Fluid Mech.* (in press).

Zeff, B. W., Kleber, B., Fineberg, J. & Lathrop, D. P., 2000, Singularity dynamics in curvature collapse and jet eruption on a fluid surface. *Nature*, **403**, 401-404.